Integrative Biology

Cite this: *Integr. Biol.*, 2011, **3**, 1011–1019

www.rsc.org/ibiology

PAPER

Microtopographical assembly of cardiomyocytes†

Anuj A. Patel,[ab] Tejal A. Desai[ac] and Sanjay Kumar*[ab]

Received 12th March 2011, Accepted 4th August 2011
DOI: 10.1039/c1ib00024a

One of the central challenges in cardiac tissue engineering is the control of the assembly and organization of functional cardiac tissue. Maintenance of a three-dimensional tissue architecture is key to myocardial function *in vivo*, and a variety of studies hint that provision of topological cues within scaffolds can facilitate the engineering of functional myocardial tissue by promoting this architecture. To explore this possibility in an isolated and well-defined fashion, we have designed scaffolds of polydimethylsiloxane (PDMS) with microtopographic pillars (''micropegs'') to provide cells with defined structures with which to interact in three dimensions. We show that these surfaces permit HL-1 cardiomyocytes to grow, form myofibrillar structures and cell–cell adhesions, and beat spontaneously. Additionally, the cells and their nuclei interact with the full length of the micropegs, indicating that the micropegs promote a three-dimensional cytoarchitecture in the context of a two-dimensional scaffold. We also show that the number of cells interacting with a micropeg can be controlled by manipulating incubation time, micropeg spatial arrangement, or micropeg diameter. Western blots reveal that the expression of the junctional markers N-cadherin and connexin 43 is upregulated in the presence of specific arrangements of micropegs, suggesting that micropegs can enhance cardiomyocyte function. Together, these data show that microtopography can be used to provide three-dimensional adhesion and control the assembly of functional cardiac tissue on a two-dimensional surface.

Introduction

The incorporation of material-encoded biophysical signals has emerged as a powerful tool for controlling cellular assembly and function in the design of tissue engineering scaffolds. At the single-cell level, control of cell shape *via* extracellular matrix (ECM) geometry has been shown to regulate cell growth and death, adhesion, and stem cell differentiation.[1–4] Modulation of the elasticity of the ECM has also been shown to regulate adhesion and migration, lineage commitment and differentiation, and contractile properties.[5–9] These ideas have also been extended to the organization of whole tissues. For example, decellularized matrices that retain three-dimensional ECM structure but completely lack cells have been successfully used as a scaffold for engineering a variety of functional tissues and organs.[10,11] Moreover, geometric patterns that promote mechanical gradients can produce spatially-ordered

[a] *The UC Berkeley – UCSF Graduate Program in Bioengineering, USA*
[b] *Department of Bioengineering, 274A Stanley Hall #1762, University of California, Berkeley, CA 94720-1762, USA. E-mail: skumar@berkeley.edu; Fax: +1 510 642 5835; Tel: +1 510 643 0787*
[c] *Department of Bioengineering and Therapeutic Sciences, University of California, San Francisco, USA*
† Electronic supplementary information (ESI) available. See DOI: 10.1039/c1ib00024a

Insight, innovation, integration

Facilitation of three-dimensional tissue architecture remains a key challenge in tissue engineering. Here we use microfabrication approaches to create patterned arrays of microtopographical cues that enable a three-dimensional cytoarchitecture of cardiomyocytes while promoting a defined lateral multicellular organization. These scaffolds support multiple key cardiomyocyte properties including beating and expression of signature molecular markers, with the latter dependent on scaffold geometry. These scaffolds also have the valuable advantage of fostering a three-dimensional architecture while retaining the high throughput, fidelity, and optical accessibility of two-dimensional scaffolds. By integrating microfabrication technology with traditional cell and molecular biology tools, such as live-cell imaging, confocal imaging, and measurement of protein expression, our study supports a potential role for microtopographical patterning in the engineering of myocardial tissue.

stem cell differentiation in the context of both two- and three-dimensional scaffolds.[12]

Whereas the majority of the field's attention has focused on the influence of substrate geometry and elasticity, scaffold microtopography has been relatively underexplored and remains poorly understood, despite the fact that it too has been shown to strongly influence cell behavior. For example, microgrooved substrates have been used to support the adhesion, alignment, and proliferation of various cell types,[13,14] and cyclic stretching of mesenchymal stem cells on these substrates enhances differentiation into vascular cells.[15] We recently showed that provision of micron-sized protrusions ("micropegs") on a two-dimensional scaffold can strongly regulate the proliferation of fibroblasts and skeletal myoblasts through a mechanism that depends on the cell's ability to generate contractile force against these protrusions.[16] Consistent with this notion, we later showed that attachment to micropegs can regulate adhesion strength, motility, and expression of contractile markers.[17]

Microtopography bears particular promise for the engineering of myocardial tissue, in which well-defined, three-dimensional lateral and transmural architectures are key to the coordinated conduction of electrical signals and efficient generation of mechanical force. For example, it has been shown that changes in intracellular levels of Ca^{2+} and increased pacemaking activity in cardiomyocytes can be controlled by the use of microgrooved scaffolds that support a three-dimensional cytoarchitecture.[18] Furthermore, microcantilever displacement measurements have shown that cardiomyocytes grown on microgrooved surfaces generate higher contractile forces than those on flat surfaces.[19] Provision of tissue-like topographic cues has also been shown to reduce cell proliferation within mixed embryonic stem cell-derived cardiomyocyte cultures prior to terminal differentiation.[20]

While these studies have helped to establish the potential relevance of microtopographical features in the design of myocardial tissue engineering scaffolds, they leave several open questions: can these design concepts, which have largely been established with either heterogeneous progenitor populations or fully differentiated primary cardiomyocytes, be translated to immortalized cardiomyocyte culture models, which are relatively homogeneous and bear interest for high-throughput screening and toxicology applications? Can microtopographical cues be spatially patterned, thereby concurrently promoting both a three-dimensional cytoarchitecture and ordered lateral assembly? Finally, does the presence of topographical cues influence the expression of markers of cardiomyocyte function and maturation? In this study, we address all of these questions through the use of newly-designed PDMS scaffolds containing microtopographical features patterned in a variety of two-dimensional configurations. We culture HL-1 cardiomyocytes[21] on these scaffolds and show that the micropatterned surfaces support growth, beating, and expression of functional cardiomyocyte markers. Confocal imaging reveals that the cardiomyocytes interact with the full vertical dimension of the micropegs, thereby adopting a three-dimensional architecture, and time lapse imaging demonstrates that the micropegs serve as preferential adhesion sites for cells, suggesting that these structures might be exploited as physical organizing centers that could facilitate the assembly of cultured cardiomyocytes into multicellular units.

Results

Geometrical arrangements of micropegs

In our previous work, we showed that inclusion of microtopographical protrusions ("micropegs") into two-dimensional scaffolds can regulate the adhesion, polarity, and migration of a variety of cultured cell types, including fibroblasts and differentiated neonatal cardiomyocytes.[16,17,22–24] In those previous studies, the micropegs were presented as simple rows, with 50 μm spacing between adjacent micropegs and 125 μm between rows, where the spacings indicate the center-to-center distance between micropegs. This arrangement was chosen to present cells enough flat space to adhere and migrate as well as to interact with one or more micropegs. In the current study, we began by asking whether this approach could be extended to micropegs arranged in more complex geometries, which in turn might enable us to better understand the relationship between micropeg spacing and cell behavior and potentially allow us to spatially pattern the cells themselves. To test the effects of the geometry of surface topography on cardiomyocyte assembly and function, we recreated the rows and also developed three other arrangements of micropegs: densely packed (50 μm × 50 μm spacing), sparsely packed (125 μm × 125 μm spacing), and clustered (50 μm between adjacent micropegs, 200 μm between clusters) (Fig. 1). The dense and sparse arrangements were chosen to further elucidate the effects of micropeg spacing on cardiomyocyte arrangement, and the clustered arrangement was chosen to determine regulatory effects of locally concentrating the micropegs. In all subsequent studies, we compared results obtained on each of these substrates to one another and to a flat PDMS surface used as a control.

Micropatterned surfaces permit growth of HL-1 cells

An important limitation of our previous studies was the use of fully differentiated neonatal cardiomyocytes, which must be freshly isolated from tissue, suffer from batch-to-batch variation, and cannot be propagated in culture. Moreover, these cells lack the throughput and self-renewal properties of cardiomyocyte progenitors desired in toxicology, drug screening, and tissue engineering and regenerative medicine applications. While defined culture systems for generating cardiomyocytes from multipotent and pluripotent stem and progenitor cells have recently begun to emerge, their use remains technically demanding, with isolation of stable cardiomyocyte progenitors proving particularly challenging.[25,26] As an alternative, a continuous culture model known as the HL-1 line was recently developed from immortalized mouse atrial cardiomyocytes that is capable of self-renewal, synchronous beating, and expresses cardiac-specific functional markers, including many proteins relevant to formation of gap junctions and other cell–cell junctional complexes. While these cells differ somewhat from primary cardiomyocytes in their electrophysiological and contractile properties, they are nonetheless finding increasing use in the modeling of myocardial disease and in pharmacological testing.[27–32] HL-1 cells are traditionally

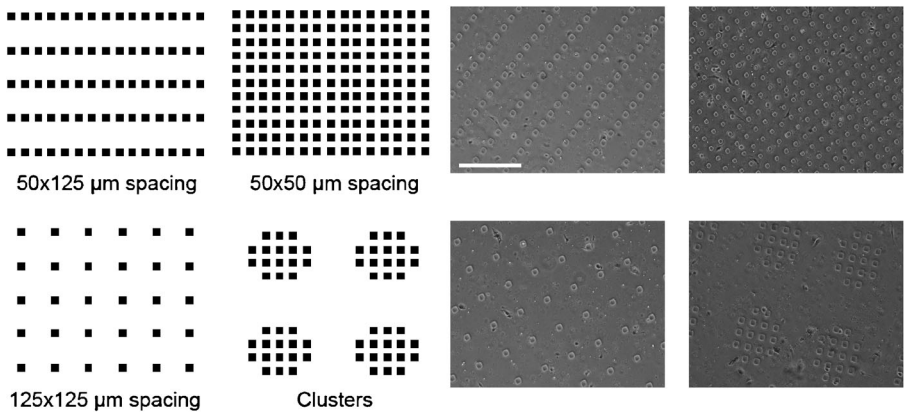

Fig. 1 Spatial arrangements of micropegs. Schematic illustrations of the four different arrangements of micropegs (left) with phase-contrast images of HL-1 cells adherent to each scaffold (right). The numbers beneath the first three arrangements represent center-to-center spacings between adjacent micropegs along each axis of the array. In the "clusters" arrangement, the center-to-center spacing between micropegs within a cluster is 50 μm and the center-to-center distance between adjacent clusters is 350 μm. Micropegs are 25 μm wide and 15 μm tall. All experiments were performed on each of these substrates as well as flat PDMS. Scale bar = 250 μm.

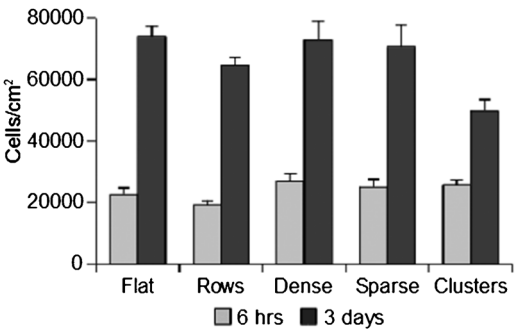

Fig. 2 Flat and patterned PDMS surfaces support the adhesion and growth of HL-1 cardiomyocytes. Cells were cultured for either 6 hours or 3 days on a specified PDMS scaffold, then fixed and fluorescently stained with DAPI, and counted using a fluorescence microscope. Cell counts were then normalized to the flat surface area available for adhesion on a given scaffold. Each condition shows significant growth from 6 hours to 3 days as measured by the Student *t*-test ($p < 0.01$). However, the differences in growth rate between conditions have not been shown to be significant. Error bars represent SEM.

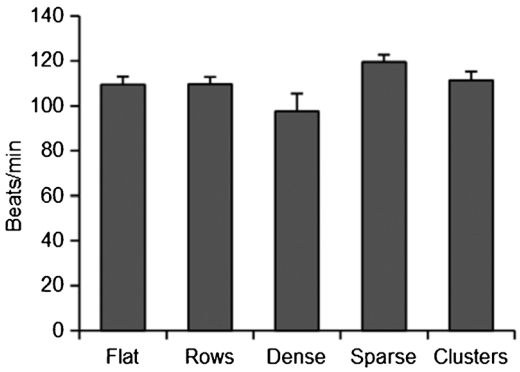

Fig. 3 HL-1 beating rates remain consistent across different patterned surfaces. HL-1 beating was visualized using time-lapse phase-contrast imaging and measured by counting the number of beats in a 60 second period. Measurements were taken once cells reached confluence, which occurred three days after seeding. Error bars represent SEM, and $p > 0.05$ across all conditions by the Student *t*-test.

grown on glass or tissue culture plastic functionalized with gelatin and fibronectin. Thus, we first asked whether PDMS with a similar coating could support adhesion and growth of HL-1 cells by culturing cells on each scaffold and counting the number of adherent cells at early and late time points after seeding, as measured by DAPI-positive nuclei (Fig. 2). All scaffolds supported attachment of HL-1 cells within 6 hours of plating, with the number of attached cells increasing at 3 days, demonstrating that cells can proliferate on all scaffolds. Exclusion of the collagen/fibronectin coating nearly completely abolished HL-1 adhesion (data not shown), indicating that the biochemical information encoded in these matrix proteins is necessary for attachment.

HL-1 cardiomyocytes spontaneously beat on PDMS surfaces

The ability to spontaneously beat in culture is a signature property of differentiated cardiomyocytes, and HL-1 cardiomyocytes have previously been shown to beat spontaneously on gelatin/fibronectin-coated glass in culture medium that contains norepinephrine. Thus, we used phase-contrast time-lapse imaging to capture beating on our scaffolds and to quantify the beating rate (Fig. 3, Movies 1–5, ESI†). Because cells were only observed to beat after reaching confluence, we performed our imaging once cultures had reached that point, which typically occurred three days after seeding (although the exact time depended on initial cell density). All scaffolds supported beating with rates in the range of 90–120 beats per minute, similar to previously-reported HL-1 beating rates.[33,34] In all cases, beating was only observed in the context of multicellular foci, implying that all scaffolds are capable of supporting mechanical and electrophysiological coupling between cells.

Ratio of cells in contact with micropegs depends upon time and the arrangement and width of micropegs

The above data establish that micropegs facilitate cardiomyocyte attachment and do not preclude the ability to form

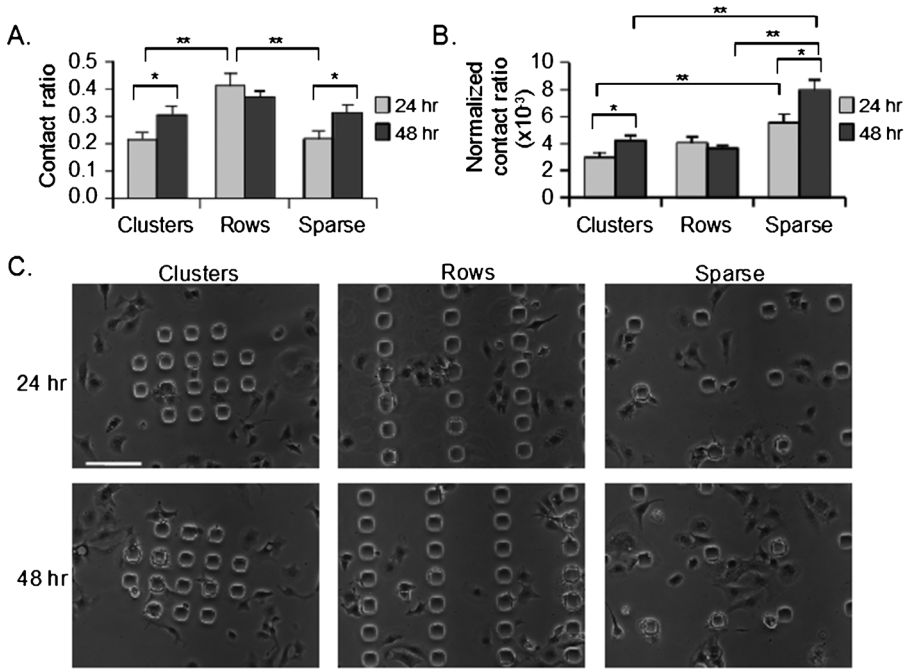

Fig. 4 Micropeg arrangement and incubation time regulate cardiomyocyte assembly. Cells were seeded on patterned substrates and analyzed after 24 or 48 hours. (A) Micropeg contact ratio on each surface at 24 and 48 hours post seeding, as defined by the ratio of cells in contact with a micropeg to the total number of cells in a field of view. Error bars represent SEM. Asterisk indicates significant difference ($p < 0.05$) and double asterisk indicates a very significant difference ($p < 0.01$). (B) Micropeg contact ratio normalized by the number of micropegs in a given field of view. Error bars represent SEM. Asterisk indicates significant difference ($p < 0.05$) and double asterisk indicates a very significant difference ($p < 0.01$). (C) Representative phase-contrast images for each condition. Scale bar = 100 μm.

cell–cell contacts needed for beating. In order to better understand the dynamics of this process, we measured the ratio of cells in contact with micropegs on each surface at both 24 hours and 48 hours after seeding (Fig. 4). The ratio of cells in contact with micropegs is quantified by counting the number of cells touching micropegs and dividing by the total number of cells per field of view. In both the clustered and sparse arrangements, this ratio increases with time, as opposed to the rows arrangement where this ratio remains constant (Fig. 4A). For the dense arrangement of micropegs, these contact ratios were, as expected, typically very close to 1, *i.e.*, all cells were in contact with a micropeg (not shown). To more closely examine the effect of differences in micropeg density available for cell adhesion, we normalized the number of micropeg-attached cells by the number of micropegs for each field of view (Fig. 4B). This revealed consistent values across all scaffolds at 24 h post-seeding, with an increase for the sparse and clustered arrangements at 48 h (Fig. 4C).

We further investigated the ability of the micropegs to control cell organization by varying the height and width of individual micropegs while keeping the arrangement of the micropegs constant. Using the sparse arrangement of micropegs, we varied the height of micropegs between 5, 15, and 50 μm, and the width of micropegs between 15, 25, and 50 μm (Fig. 5). We observed that the contact ratio did not vary significantly with micropeg height but did rise with increasing micropeg width, as expected, given that wider micropegs provide additional surface area for attachment (Fig. 5A). Consistent with our observations with standard-sized micropegs (Fig. 4) contact ratios in all cases increased from 24 to 48 hours. When these values were normalized to the width of the micropegs, we found that some of the effects of the increasing width on the contact ratio were washed out, but that the normalized ratio for the narrower micropegs was slightly higher for each height (Fig. 5B).

Taken together, these data are consistent with a kinetic model in which cells initially adhere to flat portions of the scaffold, encounter micropegs as they migrate, and preferentially adhere to these structures over time. In other words, even for scaffolds in which a small minority of the available adhesive area is occupied by micropegs, these micropegs eventually retain and sequester a disproportionate number of cardiomyocytes.

HL-1 cells exhibit myofibrillar structures and cell–cell adhesions and interact with the full length of the micropegs

As described earlier, a key design advantage of micropeg-based scaffolds is that they are expected to promote a three-dimensional cytoarchitecture that is more representative of cellular morphology in tissue and is critically tied to coordination of function. To assess the degree to which our scaffolds promote three-dimensional topologies, we used confocal microscopy to visualize the expression and subcellular localization of the cardiac-specific myosin heavy chain, which also serves as a secondary marker of cardiomyocyte function (Fig. 6). For all scaffolds, cardiomyocytes expressed cardiac-specific myosin robustly, with localization reflecting myofibril

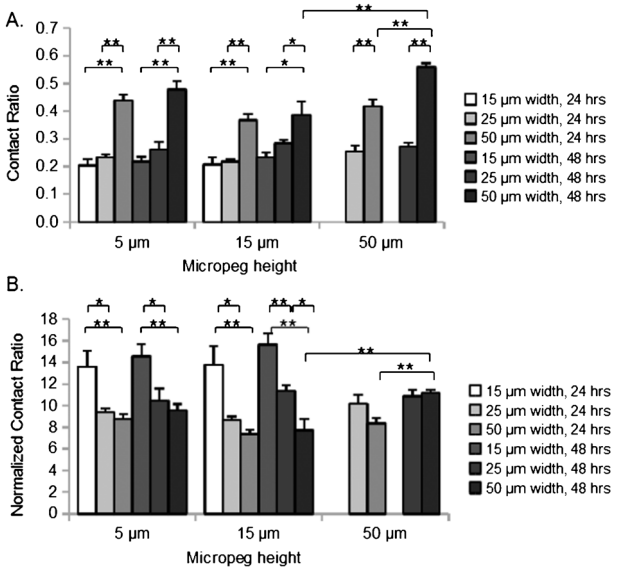

Fig. 5 Cardiomyocyte assembly depends on micropeg width but not height. Cells were seeded on "sparse" patterned substrates with micropegs of varying height and width and analyzed after 24 and 48 hours. (A) Micropeg contact ratio on each surface at 24 and 48 hours post-seeding, as defined by the ratio of cells in contact with a micropeg to the total number of cells in a field of view. Error bars represent SEM. Asterisk indicates significant difference ($p < 0.05$) and double asterisk indicates a very significant difference ($p < 0.01$). (B) Micropeg contact ratio normalized by the width of the micropegs. Note that data for the tallest and thinnest micropegs (15 μm width, 50 μm height) are absent because the high fragility of these structures precluded their robust fabrication and manipulation in culture.

assembly. Cells frequently wrapped themselves around the micropegs, with cell nuclei flattened against the micropeg walls. For dense scaffolds and scaffolds arrayed as rows and clusters, cells were sometimes observed to bridge adjacent micropegs. Optical sectioning revealed that the cardiomyocytes also interacted with the full height of the micropegs, consistent with adoption of a three-dimensional architecture. To investigate scaffold effects on cell–cell adhesion, we immunostained and performed confocal imaging against N-cadherin (Fig. 7). Clear localization of this marker to cell–cell interfaces was observed across all scaffolds. Curiously, N-cadherin was also observed at the cell–micropeg interface, although it is unclear whether this represents ectopic localization to cell-matrix contacts or merely reflects the projection of nonspecific N-cadherin staining across multiple horizontal planes. As with myosin, N-cadherin staining was observed along the entire length of the micropeg, supporting the notion that the cells engage the full vertical aspect of these structures and thereby maintain a three-dimensional architecture.

N-cadherin and connexin 43 expression can be controlled by micropeg arrangement

Having shown that the micropeg surfaces can regulate the cytoarchitecture of the cardiomyocytes without compromising beating, we next sought to quantify the extent to which micropegs could be used to quantitatively regulate expression of functional markers. We focused on the cell–cell adhesion proteins N-cadherin and connexin 43, the former serving as an early marker of cell–cell structural/mechanical coupling and the latter serving as a later marker of cell–cell electrical coupling (Fig. 8).[35] Western blots revealed comparable expression levels of both markers across all scaffolds, with modest (10–30%) but statistically significant increases in N-cadherin expression on dense and clustered substrates and in connexin-43 expression on row and dense substrates. Importantly, inclusion of micropegs did not reduce expression of either marker, consistent with the notion that the presence of these structures does not compromise cardiomyocyte function.

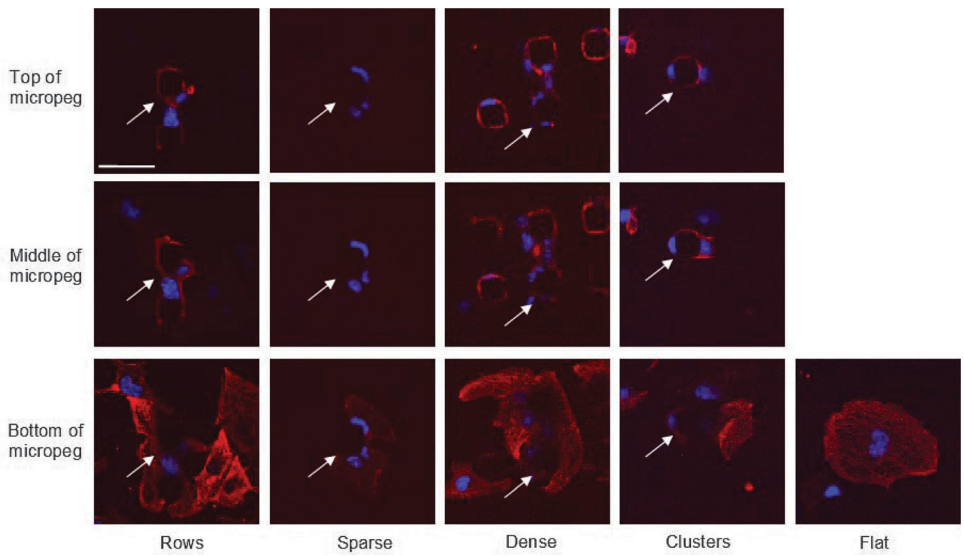

Fig. 6 myosin heavy chain is expressed along the full length of the micropegs and incorporates into myofibrils. HL-1 cells were cultured for 3 days, fixed and immunostained for the myosin heavy chain (red) and DAPI (blue) and imaged with a confocal microscope. Images were taken at three positions for each condition: the flat surface of the PDMS, the vertical midpoint of the micropeg, and the top of the micropeg. For completely flat PDMS, images were taken at the surface. White arrows indicate the location of one micropeg within the field of view. Scale bar = 50 μm.

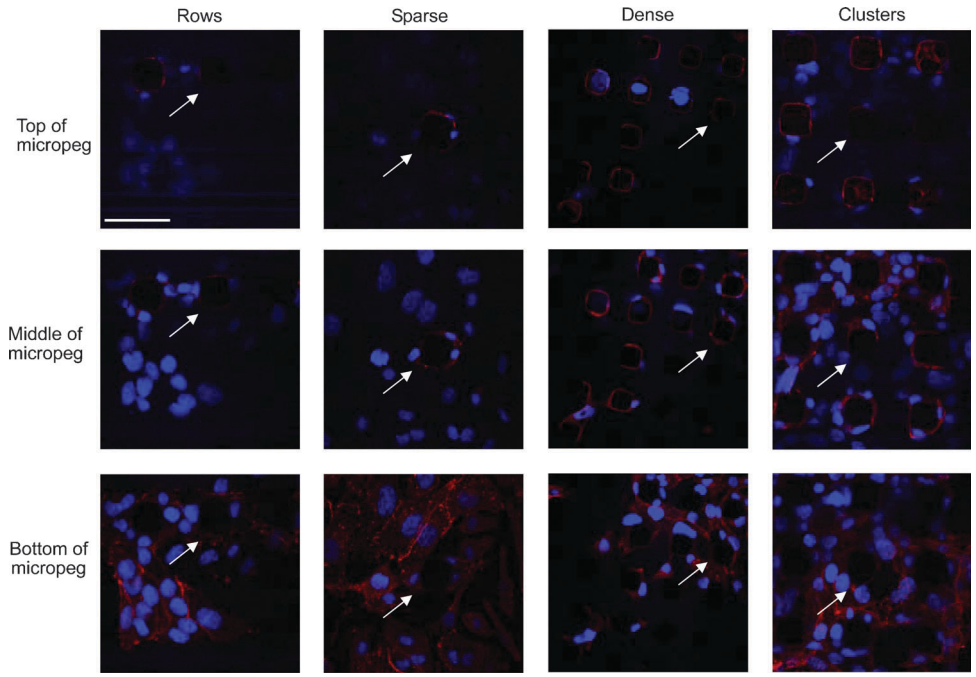

Fig. 7 Scaffold microtopography affects N-cadherin expression. HL-1 cells were cultured for 3 days, fixed and immunostained for N-cadherin (red) and DAPI (blue) and imaged with a confocal microscope. Images were taken at three positions for each condition: the flat surface of the PDMS, the vertical midpoint of the micropeg, and the top of the micropeg. White arrows indicate the location of one micropeg within the field of view. Scale bar = 50 μm.

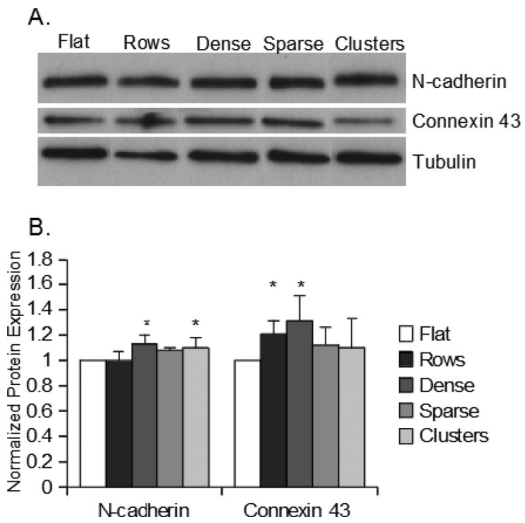

Fig. 8 Expression of cell–cell junctional proteins depends on the spatial arrangement of micropegs. (A) Representative Western blot of protein expression of cell–cell adhesion junction proteins N-cadherin and connexin 43 and loading control tubulin on each patterned PDMS substrate. Cells were seeded onto each substrate and lysates were collected after 72 hours. (B) Ratio of protein expression of N-cadherin and connexin 43 on each patterned PDMS substrate to that on a flat substrate after 72 hours. Expression levels were normalized to the expression of tubulin on each surface. Errors bars represent SEM. Asterisk indicates significant difference from expression on flat PDMS ($p < 0.05$).

Discussion

We have used live cell time lapse imaging, confocal fluorescence microscopy, and analysis of protein expression to investigate the role played by microtopographical cues in controlling the adhesion, organization, and function of cardiomyocytes. We find that these micropegs can be patterned in specific geometric arrangements that can in turn promote sequestration of cardiomyocytes into specific macro-architectures on the scaffold. Inclusion of these micro-topographical features does not compromise cardiomyocyte function as measured by beating rate and expression and localization of specific functional markers. Attachment to a micropeg also promotes adoption of a three-dimensional morphology in which cardiomyocytes associate with the lateral walls of the micropeg. Combined with our previous work detailing increased cell adhesion strength to micropegs compared to flat surfaces, these results support a model in which micropegs serve as organizing centers that recruit and retain cardiomyocytes over time and could potentially serve as nucleating sites for the assembly of functional clusters of cardiac tissue.

A significant new finding of this study is that the arrangement of the micropegs determines how likely the cardiomyocytes are to attach to them. For all the patterns, the ratio of cells in contact with micropegs is greater than one would expect to occur through random distribution of cells on the surface. This is most pointedly illustrated by the fact that the pattern with the lowest global density of micropegs was the one with the highest ratio of cells contacting micropegs. The preferential attachment of cardiomyocytes to micropegs leads to increased clustering, three-dimensional cellular organization, and changes in the localization and orientation of the nucleus. These changes suggest that cellular organization can be controlled by modulating the arrangement of the microtopographical features. While the degree of cell patterning observed here is relatively modest, one could envision

enhancing this effect by creating haptotactic or durotactic cues on the scaffold that promote migration to the topographical features. Moreover, the micropegs themselves conceivably could be chemically functionalized with specific adhesive ligands or even used as depots for the controlled release of differentiation factors. Future efforts will focus on incorporating these functionalities.

Our studies reveal that incorporation of micropegs into scaffolds does not compromise, and in some cases may modestly enhance, expression of N-cadherin and connexin-43, two markers of cardiac maturation. These two proteins cooperate to propagate mechanical and electrical signals that underlie synchronous beating of cardiac tissue.[35] Developmentally, N-cadherin expression precedes connexin 43 expression in the fetal heart and is a prerequisite for the formation of gap junctions in the intercalated disk.[36,37] N-cadherin is also important for the anchoring of myofibrils and the transmission of force from cell to cell, and N-cadherin dependent mechanosensing has been shown to be a regulator of cardiomyocyte shape, myofibrillar organization, and cortical stiffness.[38,39] Loss of N-cadherin expression has been linked to the development of myocardial arrhythmia due to slowed conduction velocity and gap junction remodeling.[40] Similarly, connexin 43 is the primary component of gap junctions and allows for the conduction of the electrical signal among neighboring cardiac cells.[35] Loss of connexin 43 expression and changes in its spatial distribution in the intercalated disc can lead to fatal cardiac arrhythmia and dysfunction.[41,42] Further study should help to determine whether scaffold geometry can be used to manipulate myocardial function *per se*, including the magnitude of force generation and the speed with which electrical signals are conducted across the scaffold surface.

These results add to a growing body of evidence supporting a role for the mechanical and topographical environments in the design of cardiac tissue engineering applications. Scaffold stiffness has previously been shown to regulate stem cell differentiation, cardiac organization, beating rate, and contractility.[6,8,43–45] Recently, a parallel set of studies has shown that the introduction of microrods into 3D cardiac tissue engineering scaffolds can be used to modulate cardiac function, scar tissue formation, and stem cell differentiation, implying that microtopographical cues can be incorporated into three-dimensional hydrogel scaffolds.[46–48] In each of these cases, the microrods are embedded in a gel scaffold oriented randomly. Based on our results, we speculate that the functionality and organization of the cardiomyocytes in these scaffolds could be further manipulated by controlling the spatial arrangement of the microrods.

Conclusions

We have demonstrated that we can promote both the three-dimensional architecture and lateral organization of cardiomyocytes through the use of microtopographical patterning. These micropatterned substrates are capable of supporting cardiomyocyte growth, beating, myofibril assembly, and expression of functional markers. These results suggest that topographical patterning may be used to control the assembly of cardiac tissue in cell culture and tissue engineering applications.

Experimental

Cell culture

HL-1 mouse cardiomyocytes were generously provided by Dr William C. Claycomb, Louisiana State University. Following established HL-1 culture protocols,[21] tissue culture flasks were prepared by precoating with a solution containing 0.02% gelatin (Fisher Scientific, Pittsburgh, PA) and 5 μg ml^{-1} fibronectin (Sigma-Aldrich, St Louis, MO) and incubating overnight at 37 °C. Cultures were maintained in these flasks in complete medium consisting of Claycomb Medium (Sigma-Aldrich) supplemented with 10% fetal bovine serum (Sigma-Aldrich), 0.1 mM norepinephrine (Sigma-Aldrich), 1× L-glutamine (Sigma-Aldrich), and 1% penicillin/streptomycin (Gibco, Carlsbad, CA). Cell cultures were stored in a humidity-controlled 5% CO_2 incubator at 37 °C. For experiments, cells were allowed to grow to confluence, trypsinized, resuspended in complete medium, and plated on PDMS scaffolds.

Fabrication of PDMS micropegs

PDMS micropeg arrays were fabricated as previously described.[16] Briefly, an SU-8 negative photoresist (PR) (Microchem, Newton, MA) was spin-coated onto a single-crystal silicon wafer and baked at 95 °C for 3 min. SU-8 2005, 2010, and 2035 were used to make thicknesses of 5, 15, and 50 μm, respectively. Microscale holes were introduced by placing a patterned photomask over the coated wafer and exposing it to UV light for 25–30 s at an intensity of 5 mW cm^{-2}, washing in an SU-8 developer (Microchem) for 30 s to remove uncrosslinked PR, then baking at 95 °C for 3 min. Different patterns were created by changing the pattern of the photomask. To create PDMS micropeg arrays, PDMS and the curing agent were prepared and mixed as directed by the manufacturer (Sylgard 184, Dow Corning, MI), degassed under vacuum, and spin-coated onto an SU-8 mold. The PDMS was baked for 1 h at 80 °C, then peeled from the SU-8 masters. Unpatterned PDMS membranes were fabricated in an identical manner. Prior to use in cell culture experiments, the PDMS was rendered hydrophilic by exposure to air plasma and then incubated with the gelatin/fibronectin mix mentioned above for 2 h at 37 °C. For experiments on PDMS surfaces with no ECM, the same procedure was followed but the gelatin/fibronectin was replaced by phosphate-buffered saline. For studies with fixed micropeg height and width, we used arrays featuring micropegs of 15 μm height and 25 μm diameter.

Growth and micropeg contact ratio measurements

Cells were plated on either glass or PDMS at a concentration of 10^4 cells ml^{-1} and were fixed with 4% paraformaldehyde (PFA) at appropriate time points. Cells were then incubated with 4′,6-diamidino-2-phenylindole (DAPI) (Invitrogen, Carlsbad, CA) for 25 min at room temperature to visualize nuclei. Cells were then visualized with a Nikon TE2000E2 epifluorescence microscope. For growth studies, the number of nuclei at each time point was quantified using ImageJ (NIH). For contact ratio studies, the numbers of nuclei were counted

manually and then compared to phase images to determine whether cells were in contact with micropegs or completely in flat space.

Beating measurements

Cells were plated on PDMS and allowed to grow to confluence. Beating cells were localized and recorded using time-lapse phase contrast imaging (Nikon TE2000E2). To quantify beating rates, individual beating foci were recorded for 30 s and the number of beats was divided by the time elapsed.

Immunostaining and confocal imaging

Cells grown on PDMS surfaces were fixed with 4% PFA at room temperature for 10 min, or with 19 : 1 ethanol : acetone at 4 °C for 15 min for the myosin heavy chain. Cells were then permeabilized, blocked with 5% normal goat serum, then incubated in mouse primary antibodies directed against either N-cadherin (BD Biosciences, San Jose, CA) diluted 1 : 100 or the sarcomeric myosin heavy chain (Developmental Studies Hybridoma Bank, Iowa City, IA) diluted 1 : 20 for 1 h, followed by incubation with DAPI and a goat anti-mouse secondary antibody conjugated to an Alexa Fluor dye (Invitrogen) for 45 min at 1 : 500 for N-cadherin and 1 : 750 for the myosin heavy chain. Confocal images were acquired with a Zeiss LSM 510 Meta Confocal Laser Scanning Microscope.

Western blotting

Cells were allowed to adhere and spread on either flat or micropeg-patterned PDMS as above, followed by trypsinization and harvest of lysate. Protein levels were determined by a Western blot using mouse primary antibodies against N-cadherin (BD Biosciences) and tubulin (Sigma-Aldrich) and a rabbit antibody against connexin 43 (Cell Signaling Technology, Danvers, MA), all diluted at 1 : 50 000 and incubated overnight at 4 °C. Bands were then detected using HRP-conjugated goat–anti-mouse and goat–anti-rabbit secondary antibodies (Invitrogen) diluted 1 : 100 000 and incubated for 45 min at room temperature, followed by development using the Novex ECL chemiluminescent substrate (Invitrogen). ImageJ was used to determine band intensity levels from the developed blots. All intensity levels were internally normalized to the tubulin loading control prior to calculating ratios of protein levels on micropeg-textured *versus* flat scaffolds. It is important to note that lysates obtained from micropeg-textured scaffolds contain protein contributions both from cells adhered to micropegs and cells adhered to the intervening flat regions. Thus, immunoblots obtained with these scaffolds necessarily *underestimate* the effects of the micropegs on protein expression relative to completely flat scaffolds.

Statistics

Results are presented as mean with error bars representing the standard error of the mean (SEM). Data were analyzed by Student's *t*-test for significance.

Acknowledgements

SK gratefully acknowledges the support of the NIH Director's New Innovator Award (1DP2OD004213), a part of the NIH Roadmap for Medical Research, and a Beginning Grant-in-Aid from the American Heart Association (0765128Y). TAD gratefully acknowledges partial support from the NIH (HL090523). We would also like to thank the Biological Imaging Facility at UC Berkeley for use of their confocal microscope.

References

1 C. S. Chen, M. Mrksich, S. Huang, G. M. Whitesides and D. E. Ingber, Geometric control of cell life and death, *Science*, 1997, **276**, 1425–1428.
2 C. J. Lee, M. S. Blumenkranz, H. A. Fishman and S. F. Bent, Controlling cell adhesion on human tissue by soft lithography, *Langmuir*, 2004, **20**, 4155–4161.
3 R. McBeath, D. M. Pirone, C. M. Nelson, K. Bhadriraju and C. S. Chen, Cell shape, cytoskeletal tension, and RhoA regulate stem cell lineage commitment, *Dev. Cell*, 2004, **6**, 483–495.
4 K. A. Kilian, B. Bugarija, B. T. Lahn and M. Mrksich, Geometric cues for directing the differentiation of mesenchymal stem cells, *Proc. Natl. Acad. Sci. U. S. A.*, 2010, **107**, 4872–4877, DOI: 10.1073/pnas.0903269107.
5 T. A. Ulrich, E. M. de Juan Pardo and S. Kumar, The mechanical rigidity of the extracellular matrix regulates the structure, motility, and proliferation of glioma cells, *Cancer Res.*, 2009, **69**, 4167–4174, DOI: 10.1158/0008-5472.CAN-08-4859.
6 A. J. Engler, S. Sen, H. L. Sweeney and D. E. Discher, Matrix elasticity directs stem cell lineage specification, *Cell*, 2006, **126**, 677–689, DOI: 10.1016/j.cell.2006.06.044.
7 K. Saha, A. J. Keung, E. F. Irwin, Y. Li, L. Little, D. V. Schaffer and K. E. Healy, Substrate modulus directs neural stem cell behavior, *Biophys. J.*, 2008, **95**, 4426–4438, DOI: 10.1529/biophysj.108.132217.
8 A. J. Engler, C. Carag-Krieger, C. P. Johnson, M. Raab, H. Y. Tang, D. W. Speicher, J. W. Sanger, J. M. Sanger and D. E. Discher, Embryonic cardiomyocytes beat best on a matrix with heart-like elasticity: scar-like rigidity inhibits beating, *J. Cell Sci.*, 2008, **121**, 3794–3802, DOI: 10.1242/jcs.029678.
9 W. A. Lam, L. Cao, V. Umesh, A. J. Keung, S. Sen and S. Kumar, Extracellular matrix rigidity modulates neuroblastoma cell differentiation and N-myc expression, *Mol. Cancer*, 2010, **9**, 35, DOI: 10.1186/1476-4598-9-35.
10 H. C. Ott, T. S. Matthiesen, S. K. Goh, L. D. Black, S. M. Kren, T. I. Netoff and D. A. Taylor, Perfusion-decellularized matrix: using nature's platform to engineer a bioartificial heart, *Nat. Med.*, 2008, **14**, 213–221, DOI: 10.1038/nm1684.
11 T. H. Petersen, E. A. Calle, L. Zhao, E. J. Lee, L. Gui, M. B. Raredon, K. Gavrilov, T. Yi, Z. W. Zhuang, C. Breuer, E. Herzog and L. E. Niklason, Tissue-engineered lungs for *in vivo* implantation, *Science*, 2010, **329**, 538–541, DOI: 10.1126/science.1189345.
12 S. A. Ruiz and C. S. Chen, Emergence of patterned stem cell differentiation within multicellular structures, *Stem Cells*, 2008, **26**, 2921–2927, DOI: 10.1634/stemcells.2008-0432.
13 Y. C. Wang and C. C. Ho, Micropatterning of proteins and mammalian cells on biomaterials, *FASEB J.*, 2004, **18**, 525–527, DOI: 10.1096/fj.03-0490fje.
14 R. B. Vernon, M. D. Gooden, S. L. Lara and T. N. Wight, Microgrooved fibrillar collagen membranes as scaffolds for cell support and alignment, *Biomaterials*, 2005, **26**, 3131–3140, DOI: 10.1016/j.biomaterials.2004.08.011.
15 K. Kurpinski, J. Chu, C. Hashi and S. Li, Anisotropic mechanosensing by mesenchymal stem cells, *Proc. Natl. Acad. Sci. U. S. A.*, 2006, **103**, 16095–16100, DOI: 10.1073/pnas.0604182103.
16 R. G. Thakar, M. G. Chown, A. Patel, L. Peng, S. Kumar and T. A. Desai, Contractility-dependent modulation of cell proliferation and adhesionby microscale topographical cues, *Small*, 2008, **4**, 1416–1424, DOI: 10.1002/smll.200701302.
17 A. A. Patel, R. G. Thakar, M. Chown, P. Ayala, T. A. Desai and S. Kumar, Biophysical mechanisms of single-cell interactions with microtopographical cues, *Biomed. Microdevices*, 2010, **12**, 287–296, DOI: 10.1007/s10544-009-9384-7.
18 L. Yin, H. Bien and E. Entcheva, Scaffold topography alters intracellular calcium dynamics in cultured cardiomyocyte

networks, *Am. J. Physiol.: Heart Circ. Physiol.*, 2004, **287**, H1276–H1285, DOI: 10.1152/ajpheart.01120.2003.
19 J. Kim, J. Park, K. Na, S. Yang, J. Baek, E. Yoon, S. Choi, S. Lee, K. Chun and S. Park, Quantitative evaluation of cardiomyocyte contractility in a 3D microenvironment, *J. Biomech.*, 2008, **41**, 2396–2401, DOI: 10.1016/j.jbiomech.2008.05.036.
20 J. K. Biehl, S. Yamanaka, T. A. Desai, K. R. Boheler and B. Russell, Proliferation of mouse embryonic stem cell progeny and the spontaneous contractile activity of cardiomyocytes are affected by microtopography, *Dev. Dyn.*, 2009, **238**, 1964–1973, DOI: 10.1002/dvdy.22030.
21 W. C. Claycomb, N. A. Lanson, Jr, B. S. Stallworth, D. B. Egeland, J. B. Delcarpio, A. Bahinski and N. J. Izzo, Jr, HL-1 cells: a cardiac muscle cell line that contracts and retains phenotypic characteristics of the adult cardiomyocyte, *Proc. Natl. Acad. Sci. U. S. A.*, 1998, **95**, 2979–2984.
22 S. Y. Boateng, T. J. Hartman, N. Ahluwalia, H. Vidula, T. A. Desai and B. Russell, Inhibition of fibroblast proliferation in cardiac myocyte cultures by surface microtopography, *Am. J. Physiol. Cell Physiol.*, 2003, **285**, C171–C182, DOI: 10.1152/ajpcell.00013.2003.
23 J. Deutsch, D. Motlagh, B. Russell and T. A. Desai, Fabrication of microtextured membranes for cardiac myocyte attachment and orientation, *J. Biomed. Mater. Res.*, 2000, **53**, 267–275.
24 D. Motlagh, S. E. Senyo, T. A. Desai and B. Russell, Microtextured substrata alter gene expression, protein localization and the shape of cardiac myocytes, *Biomaterials*, 2003, **24**, 2463–2476.
25 Z. Melkoumian, J. L. Weber, D. M. Weber, A. G. Fadeev, Y. Zhou, P. Dolley-Sonneville, J. Yang, L. Qiu, C. A. Priest, C. Shogbon, A. W. Martin, J. Nelson, P. West, J. P. Beltzer, S. Pal and R. Brandenberger, Synthetic peptide–acrylate surfaces for long-term self-renewal and cardiomyocyte differentiation of human embryonic stem cells, *Nat. Biotechnol.*, 2010, **28**, 606–610, DOI: 10.1038/nbt.1629.
26 S. T. Wall, C. C. Yeh, R. Y. Tu, M. J. Mann and K. E. Healy, Biomimetic matrices for myocardial stabilization and stem cell transplantation, *J. Biomed. Mater. Res., Part A*, 2010, **95**, 1055–1066, DOI: 10.1002/jbm.a.32904.
27 D. B. Sanders, D. F. Larson, K. Hunter, M. Gorman and B. Yang, Comparison of tumor necrosis factor-alpha effect on the expression of iNOS in macrophage and cardiac myocytes, *Perfusion*, 2001, **16**, 67–74.
28 B. J. Brundel, H. H. Kampinga and R. H. Henning, Calpain inhibition prevents pacing-induced cellular remodeling in a HL-1 myocyte model for atrial fibrillation, *Cardiovasc. Res.*, 2004, **62**, 521–528, DOI: 10.1016/j.cardiores.2004.02.007.
29 M. E. Hensler, S. Miyamoto and V. Nizet, Group B streptococcal beta-hemolysin/cytolysin directly impairs cardiomyocyte viability and function, *PLoS One*, 2008, **3**, e2446, DOI: 10.1371/journal.pone.0002446.
30 U. Hellman, L. Malm, L. P. Ma, G. Larsson, S. Morner, M. Fu, A. Engstrom-Laurent and A. Waldenstrom, Growth factor PDGF-BB stimulatescultured cardiomyocytes to synthesize the extracellular matrix component hyaluronan, *PLoS One*, 2010, **5**, e14393, DOI: 10.1371/journal.pone.0014393.
31 T. Budde, J. Haney, S. Bien, M. Schwebe, A. Riad, C. Tschope, A. Staudt, G. Jedlitschky, S. B. Felix, H. K. Kroemer and M. Grube, Acute exposure to doxorubicin results in increased cardiac P-glycoprotein expression, *J. Pharm. Sci.*, 2011, **100**, 3951–3958.
32 M. Poteser, H. Schleifer, M. Lichtenegger, M. Schernthaner, T. Stockner, C. O. Kappe, T. N. Glasnov, C. Romanin and K. Groschner, PKC-dependent coupling of calcium permeation through transient receptor potential canonical 3 (TRPC3) to calcineurin signaling in HL-1 myocytes, *Proc. Natl. Acad. Sci. U. S. A.*, 2011, **108**, 10556–10561.
33 Z. Yang and K. T. Murray, Ionic mechanisms of pacemaker activity in spontaneously contracting atrial HL-1 cells, *J. Cardiovasc. Pharmacol.*, 2011, **57**, 28–36, DOI: 10.1097/FJC.0b013e3181fda7c4.
34 C. H. George, G. V. Higgs and F. A. Lai, Ryanodine receptor mutations associated with stress-induced ventricular tachycardia mediate increased calcium release in stimulated cardiomyocytes, *Circ. Res.*, 2003, **93**, 531–540, DOI: 10.1161/01.RES.0000091335.07574.86.
35 M. Noorman, M. A. van der Heyden, T. A. van Veen, M. G. Cox, R. N. Hauer, J. M. de Bakker and H. V. van Rijen, Cardiac cell–cell junctions in health and disease: Electrical *versus* mechanical coupling, *J. Mol. Cell. Cardiol.*, 2009, **47**, 23–31, DOI: 10.1016/j.yjmcc.2009.03.016.
36 H. Reinecke, M. Zhang, T. Bartosek and C. E. Murry, Survival, integration, and differentiation of cardiomyocyte grafts: a study in normal and injured rat hearts, *Circulation*, 1999, **100**, 193–202.
37 S. Kostin, S. Hein, E. P. Bauer and J. Schaper, Spatiotemporal development and distribution of intercellular junctions in adult rat cardiomyocytes in culture, *Circ. Res.*, 1999, **85**, 154–167.
38 Y. Luo and G. L. Radice, Cadherin-mediated adhesion is essential for myofibril continuity across the plasma membrane but not for assembly of the contractile apparatus, *J. Cell Sci.*, 2003, **116**, 1471–1479.
39 A. Chopra, E. Tabdanov, H. Patel, P. A. Janmey and J. Y. Kresh, Cardiac myocyte remodeling mediated by N-cadherin-dependent mechanosensing, *Am. J. Physiol.: Heart Circ. Physiol.*, 2011, **300**, H1252–H1266, DOI: 10.1152/ajpheart.00515.2010.
40 J. Li, V. V. Patel, I. Kostetskii, Y. Xiong, A. F. Chu, J. T. Jacobson, C. Yu, G. E. Morley, J. D. Molkentin and G. L. Radice, Cardiac-specific loss of N-cadherin leads to alteration in connexins with conduction slowing and arrhythmogenesis, *Circ. Res.*, 2005, **97**, 474–481, DOI: 10.1161/01.RES.0000181132.11393.18.
41 M. S. Spach, J. F. Heidlage, P. C. Dolber and R. C. Barr, Electrophysiological effects of remodeling cardiac gap junctions and cell size: experimental and model studies of normal cardiac growth, *Circ. Res.*, 2000, **86**, 302–311.
42 M. R. Abraham, C. A. Henrikson, L. Tung, M. G. Chang, M. Aon, T. Xue, R. A. Li, B. O' Rourke and E. Marban, Antiarrhythmic engineering of skeletal myoblasts for cardiac transplantation, *Circ. Res.*, 2005, **97**, 159–167, DOI: 10.1161/01.RES.0000174794.22491.a0.
43 K. Shapira-Schweitzer and D. Seliktar, Matrix stiffness affects spontaneous contraction of cardiomyocytes cultured within a PEGylated fibrinogen biomaterial, *Acta Biomater.*, 2007, **3**, 33–41, DOI: 10.1016/j.actbio.2006.09.003.
44 B. Bhana, R. K. Iyer, W. L. Chen, R. Zhao, K. L. Sider, M. Likhitpanichkul, C. A. Simmons and M. Radisic, Influence of substrate stiffness on the phenotype of heart cells, *Biotechnol. Bioeng.*, 2010, **105**, 1148–1160, DOI: 10.1002/bit.22647.
45 A. Marsano, R. Maidhof, L. Q. Wan, Y. Wang, J. Gao, N. Tandon and G. Vunjak-Novakovic, Scaffold stiffness affects the contractile function of three-dimensional engineered cardiac constructs, *Biotechnol. Prog.*, 2010, **26**, 1382–1390, DOI: 10.1002/btpr.435.
46 M. W. Curtis, S. Sharma, T. A. Desai and B. Russell, Hypertrophy, gene expression, and beating of neonatal cardiac myocytes are affected by microdomain heterogeneity in 3D, *Biomed. Microdevices*, 2010, **12**, 1073–1085, DOI: 10.1007/s10544-010-9461-y.
47 P. Ayala, J. I. Lopez and T. A. Desai, Microtopographical cues in 3D attenuate fibrotic phenotype and extracellular matrix deposition: implications for tissue regeneration, *Tissue Eng. A*, 2010, **16**, 2519–2527, DOI: 10.1089/ten.TEA.2009.0815.
48 J. M. Collins, P. Ayala, T. A. Desai and B. Russell, Three-dimensional culture with stiff microstructures increases proliferation and slows osteogenic differentiation of human mesenchymal stem cells, *Small*, 2010, **6**, 355–360, DOI: 10.1002/smll.200901757.